Fracture Mechanics of Concrete and Concrete Structures -
Recent Advances in Fracture Mechanics of Concrete - B. H. Oh, et al.(eds)

Combining finite/discrete element models: a post-processing tool for fine cracks in concrete structures

B. Richard
University Paris-Est, Laboratoire Central des Ponts et Chaussées, France

A. Delaplace & F. Ragueneau
LMT-Cachan, ENS-Cachan/CNRS/Univ Paris 6./PRES UNIVERSUD Paris, France

C. Cremona
Directorate for research and innovation, Ministry of Ecology, Energy, Sustainable Development, France

ABSTRACT: Recently, efficient and very sophisticated numerical approaches have been developed in order to deal with crack propagation problems. They allow providing quantitative information related to crack opening and path. Although they are robust and rigorously formulated, their computational costs prevent to apply them on large scale structures. In this paper, authors are proposing simple and robust numerical process for obtaining quantitative information about cracks' opening. A coupled discrete-continuous numerical analysis is presented and helps to provide such a quantitative description for a reinforced concrete structure subjected to external loading. The complete RC structure is studied through a macroscopic damage-based continuous model. This level of computation helps to identify the critical parts of the structure where the density of cracks is the largest. Using this pre-calculated displacement field as boundary conditions, a discrete element approach is carried out. This provides the computation of the direction and the opening of the different cracks. A basic example highlights the relevancy of the proposed approach and encourages further works.

1 INTRODUCTION

The determination of a quantitative crack pattern stays an opened question in the field of computational mechanics. During the last decades, very accurate and sophisticated numerical methods were developed and are able to correctly manage a displacement discontinuity for representing crack propagation. Among them, the Extended Finite Element Method (Moës *et al.* 1999) and the Strong Discontinuity Method (Oliver *et al.* 1996) are the most well known. Nevertheless these techniques are rarely used for large scale applications since they require large computational resources. So far, engineers are still missing techniques to get quantitative information about crack scales.

This paper presents results from the French research project CEOS.fr which aims to assess the capability of damage mechanics based models to predict accurately and quantitatively cracking patterns for some typical reinforced concrete structures (RC beams, RC bootstrap …). The purpose of the present study is therefore to show how the classical models based on continuum damage mechanics may still provide quantitative information about cracking distribution in the case of a concrete structure. The considered concrete structure is a specimen tested in tension: the experimental results are available in the literature (Boulay *et al.* 2009). Two separate numerical analyses are performed to explore their efficiency. First, a three dimensional non linear finite element analysis based on damage mechanics is introduced. From the damage pattern and the nodal displacement field, quantitative information can be obtained. Second, in order to evaluate the correlation between the isotropic damage variable and the mean crack opening, a discrete analysis is carried out. The discrete element method is here employed for post-processing, focusing the analysis on the most critical parts of the structure.

In a first part, the approach relying on continuum damage mechanics is presented. The second part of the paper is focused on the presentation of the discrete element modeling. In the last part, the coupling of the two approaches is detailed and applied on a simple case study.

2 CONTINUUM DAMAGE MODEL

To simplify the analysis, the cracked behaviour is assumed to be split into two independent behaviours

(Pensée *et al.* 2002). For the hydrostatic strain mechanism, only cracks' openings and closings are considered. The frictional sliding is only considered for the deviatoric part of the strain and stress tensors. Experimental observations from triaxial machine tests on concrete-like materials show a direct relation between the occurrence of hysteretic loops in the materials and the ratio of hydrostatic stresses over deviatoric ones (Gabet *et al.* 2008). These results justify the decomposition of the strain energy into two different parts respectively due to the spherical and the deviatoric components. This feature is one of the key points for taking into account damage and internal sliding.

2.1 *A consistent state potential*

Most of the quasi-brittle materials, such as concrete, are subject to unilateral effects. They classically appear when the material is subject to a tension–compression loading path. It can be observed that crack closing is expressed by a gain of stiffness during the compressive phase. For numerical robustness, a scalar damage variable is chosen. Nevertheless, a major drawback lies in the difficulty to take into account total unilateral effects when a single damage variable is considered: during a tension–compression loading path, the elastic modulus is not fully recovered but only partially.

Sliding is susceptible to occur between the cracks' lips and therefore friction has to be included. This effect is exhibited when the material is subject to a cyclic loading. In order to take into account this mechanism, the approaches proposed by (Ragueneau *et al.* 2000) have been considered. Nevertheless, in the present study, it is considered that the energy rate (related to sliding) only affects the deviatoric part of the free energy. This consideration is justified because sliding and friction are mainly in relation with shear stresses. This hypothesis is consistent with the fact that in mode I cracking (pure opening), friction and sliding do not occur.

The thermodynamic potential function takes the following form:

$$\rho\Psi = \frac{1}{2}\left\{\frac{\kappa}{3}\Big((1-d) < \varepsilon_{kk} >_+^2 - < -\varepsilon_{kk} >_+^2\Big) + 2(1-d)\mu\varepsilon_{ij}^D\varepsilon_{ij}^D + 2d\mu\left(\varepsilon_{ij}^D - \varepsilon_{ij}^\pi\right)\left(\varepsilon_{ij}^D - \varepsilon_{ij}^\pi\right) + \gamma\alpha_{ij}\alpha_{ij}\right\} + H(z) \tag{1}$$

where ρ is the material density, κ and μ are the bulk and shear coefficients. ε_{ij} is the second order total strain tensor, δ_{ij} is the second order Kronecker's tensor and d is the scalar damage variable (0 for virgin material and 1 for failed material). ε_{ij}^π is the second order sliding tensor, γ is a material parameter, α_{ij} is the second order tensor associated to the kinematics hardening, z is the internal variable corresponding to the isotropic hardening and H its consolidation function. $< A_{ij} >_+$ stands for the positive part of the tensor A_{ij}, $\varepsilon_{ij}^D = \varepsilon_{ij} - \frac{1}{3}\varepsilon_{kk}\delta_{ij}$ is the second order deviatoric total strain tensor. From the state potential function, the state laws are obtained by simple derivation. The Cauchy's and frictional stress tensors are given by:

$$\sigma_{ij} = \frac{\partial\rho\Psi}{\partial\varepsilon_{ij}} = \frac{\kappa}{3}\big((1-d) < \varepsilon_{kk} >_+ - < -\varepsilon_{kk} >_+\big)\delta_{ij} + 2(1-d)\mu\varepsilon_{ij}^D + 2d\mu\left(\varepsilon_{ij}^D - \varepsilon_{ij}^\pi\right)$$

$$\sigma_{ij}^\pi = -\frac{\partial\rho\Psi}{\partial\varepsilon_{ij}^\pi} = 2d\mu\left(\varepsilon_{ij}^D - \varepsilon_{ij}^\pi\right) \tag{2}$$

The damage energy release rate is written:

$$Y = -\frac{\partial\rho\Psi}{\partial d} = \frac{1}{2}\left\{\frac{\kappa}{3} < \varepsilon_{kk} >_+^2 + 2\mu\varepsilon_{ij}^D\varepsilon_{ij}^D - 2\mu\left(\varepsilon_{ij}^D - \varepsilon_{ij}^\pi\right)\left(\varepsilon_{ij}^D - \varepsilon_{ij}^\pi\right)\right\} \tag{3}$$

The thermodynamic forces related to kinematic and isotropic hardenings can be expressed by the Equations:

$$X_{ij} = \frac{\partial\rho\Psi}{\partial\alpha_{ij}} = \gamma\alpha_{ij}; \quad Z = \frac{\partial\rho\Psi}{\partial z} = \frac{dH(z)}{dz} \tag{4}$$

where X_{ij} denotes the second order back stress tensor of the kinematic hardening and Z the thermodynamic force of the isotropic hardening.

2.2 *Damage and sliding threshold*

A damage variable is associated with the isotropic hardening variable in order to ensure that damage mechanism is not activated during unloading. The second order sliding tensor is conversely associated with the kinematics hardening variable. It allows an efficient control of the energy released during cyclic loadings. A threshold surface, denoted f_d, is introduced:

$$f_d = \bar{Y} - (Y_0 + Z) \tag{5}$$

where $\bar{Y}$ denotes energy-type variable driving damage and Y_0, an initial threshold. To define a different behaviour in tension and in compression, this variable is decomposed into direct (tension) and induced (compression) extension mechanisms:

$$\overline{Y} = \beta Y_{\text{Dir}} + Y_{\text{Ind}}$$

$$Y_{\text{Dir}} = \frac{1}{2}\varepsilon_{ij}^{\text{Dir}} E_{ijkl} \varepsilon_{kl}^{\text{Dir}} \; ; Y_{\text{Ind}} = \frac{1}{2}\varepsilon_{ij}^{\text{Ind}} E_{ijkl} \varepsilon_{kl}^{\text{Ind}} \tag{6}$$

where E_{ijkl} is the Hook's tensor with elastic parameters κ and μ. β is a parameter driving the dissymmetry of the threshold surface between tension and compression. The direct and induced extensions tensors are obtained through the following decompositions:

$$\varepsilon_{ij}^{\text{Dir}} = < \varepsilon_{ij} >_{+} \text{H}(< \varepsilon_{ij} >_{+} < \sigma_{ij} >_{+}) \; ; \quad \varepsilon_{ij}^{\text{Ind}} = \varepsilon_{ij} - \varepsilon_{ij}^{\text{Dir}} \tag{7}$$

A surface without any threshold is introduced in order to manage a sliding mechanism from kinematics hardening. It takes the form of a Von Mises's criterion (without hydrostatic effects):

$$f_{\pi} = \sqrt{\frac{3}{2}(s_{ij} - X_{ij})(s_{ij} - X_{ij})} \tag{8}$$

where s_{ij} stands for the deviatoric part of the frictional stress tensor.

2.3 *Evolution laws*

The evolution of damage and isotropic hardening variables are postulated as being associated. From the maximum dissipation principle, a unique Lagrange's multiplier, denoted $\dot{\lambda}_d$, is introduced:

$$\dot{d} = \dot{\lambda}_d \frac{\partial f_d}{\partial \overline{Y}} = \dot{\lambda}_d \; ; \dot{z} = \dot{\lambda}_d \frac{\partial f_d}{\partial Z} = -\dot{\lambda}_d \tag{9}$$

In order to keep a unique damage variable in tension and in compression, the dissymmetry between tension and compression responses can be obtained by choosing an appropriate continuously differentiable consolidation function:

$$\frac{dH(z)}{dz} = \frac{-1}{1+z}\left(\frac{\text{H}(< \varepsilon_{ij} >_{+} < \sigma_{ij} >_{+})}{A_{\text{Dir}}} + \frac{1 - \text{H}(< \varepsilon_{ij} >_{+} < \sigma_{ij} >_{+})}{A_{\text{Ind}}} \right) \tag{10}$$

where A_{Dir} and A_{Ind} are brittleness parameters for tension and compression.

Concerning friction and sliding, the flow rules are supposed not to be associated. From the maximum dissipation principle, they can be expressed as:

$$\dot{\varepsilon}_{ij}^{\pi} = \dot{\lambda}_{\pi} \frac{\partial \varphi_{\pi}}{\partial \sigma_{ij}^{\pi}} \; ; \dot{\alpha}_{ij} = -\dot{\lambda}_{\pi} \frac{\partial \varphi_{\pi}}{\partial X_{ij}} \tag{11}$$

where φ_{π} is a pseudo potential function for dissipation and $\dot{\lambda}_{\pi}$ the associated Lagrange's multiplier. It has been chosen according to (Armstrong & Frederick 1966) and can be expressed as:

$$\varphi_{\pi} = \sqrt{\frac{3}{2}(s_{ij} - X_{ij})(s_{ij} - X_{ij})} + \frac{a}{2} X_{ij} X_{ij} \tag{12}$$

It allows overcoming the main linearity drawback of the Drucker's criterion for associated hardenings. Let us note that this approach ensures that the sliding tensor, the kinematics hardening tensor and the back stress tensor are pure deviatoric second order tensors.

2.4 *Strain softening and mesh dependency*

A nonlocal approach (Pijaudier-Cabot *et al.* 1987) is used as regularization technique. It consists in averaging the damage threshold surface in the vicinity of the current Gauss' point. Applied to the proposed constitutive Equations, the local damage energy released rate $\overline{Y}$ is replaced by the nonlocal one $\overline{Y}^{nl}$:

$$\overline{Y}^{nl}(x) = \frac{\int_{\Omega(x)} W(x-s)\overline{Y}(s)ds}{\int_{\Omega(x)} W(x-s)ds} \tag{13}$$

where x denotes the Gauss' point, W is a weight function (a Gaussian function usually) and $\Omega(x)$ denotes a neighbourhood around x. The definition of such a domain requires the introduction of an internal length denoted l_c.

2.5 *Local responses*

The local response under cyclic loading is presented in the Figure 1, using data from Table 1.

Table1. Material parameters used for the concrete model.

Material parameters		Values
Young modulus	E	36000 MPa
Poisson's ratio	ν	0.2
Initial threshold	Y_0	200 Jm^{-3}
Brittleness in tension	A_{Dir}	1.6 10^{-3} Pa^{-1}
Brittleness in compression	A_{Ind}	1.6 10^{-5} Pa^{-1}
Kinematics hardening	γ_0	7.0 10^{9} Pa
Non linear hardening	a_0	5.0 10^{-7} Pa^{-1}
Dissymmetry parameter	β	100

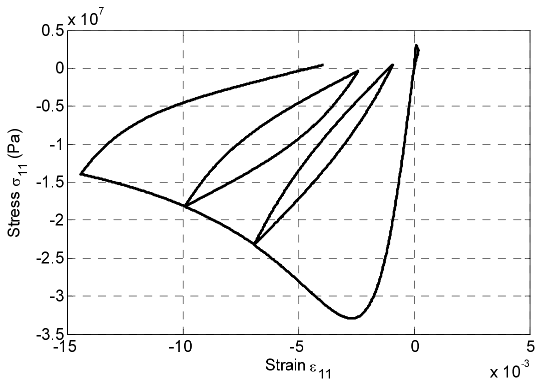

Figure 1. Damage, permanent strain and hysteretic loops for a concrete model in uniaxial tension-compression.

3 DISCRETE MODELING

A particle-based discrete model is used for fine crack description. The material is described as a particle assembly, and a crack is naturally obtained if a bond between two particles breaks. A Voronoi tessellation is used as efficient and easy mesh generation. The particle nuclei are randomly generated on a grid (Mourkazel *et al.* 1992) in order to control the boundary conditions (see Fig. 2).

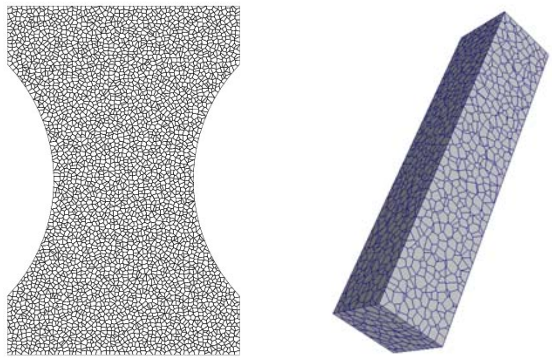

Figure 2. A 2D mesh (left) and a 3D one (right).

3.1 *Cohesion forces*

Cohesion forces can be modeled by springs at the interface of neighbored particles or by beams linking the nuclei of the particles. Here Euler-Bernoulli beams have been used. Four parameters have to be identified: the length, the area, the inertia and the elastic modulus of the beam (Schlangenand *et al.* 1997, Van Mier *et al.* 2002). The first two parameters are imposed by the mesh geometry. The two last parameters are identified in order to obtain the elastic properties of the Young modulus and the Poisson coefficient, E and ν (Delaplace *et al.* 2007). Let us note that if necessary, one can compute contact forces between unlinked particles, for example for cyclic loading with crack opening and closing.

3.2 *Nonlinear behaviour*

The nonlinear behavior of the material is obtained by considering a brittle behavior for the beams. The simplicity of this behavior is meaningful because the model represents the material at a mesoscale, where just a simple phenomenon, a crack opening in mode I, is represented. The breaking threshold P_{ij} depends on the beam strain and on the rotations of the particles (respectively i and j) linked by the beam:

$$P_{ij}\left(\frac{\varepsilon_{ij}}{\varepsilon_{cr}},\frac{\theta_{ij}}{\theta_{cr}}\right)>1 \tag{14}$$

The critical strain ε_{cr} is identified by fitting the material tensile strength. Then, the critical rotation θ_{cr} is identified by fitting the material compression strength. Note that if the threshold depends only on the beam strain, the material compression strength is overestimated by the model. With this simple beam behavior, one can obtain a reliable description of the material behavior, either for uniaxial loadings or biaxial ones (Delaplace 2009).

3.3 *Crack description*

The study is focused on a fine description of the crack pattern, and on the measurement of the crack opening. The crack pattern is nothing else than the location of the broken beams. An example is given on figure 3 for a 2D case, where the interfaces corresponding to the broken beams are plotted.

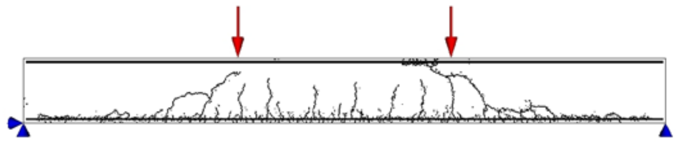

Figure 3. A crack pattern obtained for a loaded reinforced concrete beam.

The opening of the crack is computed by considering the relative displacement $(u_i - u_j)$ of the unlinked particles i and j. This approximation is justified since the particles are rigid and the material is unloaded close to the crack lips. The amplitude of the opening is projected on the direction orthogonal to the crack direction:

$$e_{ij}=\left\langle \left(u_i-u_j\right)n_{ij}\right\rangle \tag{15}$$

where $<x>=\max(x,0)$. n_{ij} stands for the normal vector used to orientate the contact between two particles i and j.

4 DISCRETE ELEMENTS AND CONTINUUM DAMAGE MODELING POST-PROCESSING

4.1 *From continuous modeling to crack growth*

4.1.1 *Framework*

To describe a crack nucleation and propagation in solid media, the most convenient approach consists in describing nonlinearities by models based on plasticity theories (Dragon *et al.* 1979), damage theory (Mazars 1984, Simo *et al.* 1987) or on smeared crack approaches (Willam *et al.* 1987).

More recent advances in numerical analysis of concrete structures promote finite element discretization by introducing material discontinuities in the finite element formulations. This enhancement may be achieved through the finite element interpolation (Belytschko *et al.* 1988, Larsson *et al.* 1996) or the finite element nodes (Oliver 1996, Belytschko *et al.* 1999, Moes *et al.* 1999).

At last, some models introduce the crack discontinuity using the discrete element method (Bazant *et al.* 1990, Bolander *et al.* 1998, d'Addetta *et al*. 2002, Delaplace *et al.* 2006). The material heterogeneity is modeled with randomized meshes and constitutive parameters. The crack nucleation and propagation are naturally accounted for in the analysis. Some recent works tends to couple the continuous and the discrete approach by employing discrete elements in the critical zones and finite element discretization in the other parts of the structures using overlapping or non overlapping numerical algorithms between two adjacent substructures (Xiao *et al.* 2003). Such an alternative imposes to know, in advance which, part of the structure requires refined and discrete analysis.

4.1.2 *Discrete element models as a post-processing numerical tool*

In the present work, the use of continuum damage mechanics at the structural level may be employed as a robust analysis of large scale structures under complex loadings. The general response in terms of displacements, strains and stresses distribution is well recovered with such analysis. But for a quantitative computation of crack openings, such an approach fails to predict local features. For this reason, another strategy is chosen in this paper. The global computation is performed using 'standard' nonlinear finite element analysis. In the post-processing phase, only the most interesting domains, requiring a refined study, will be analyzed through a discrete element approach in order to obtain some local and singular information such as crack patterns and openings. The analysis will be carried out in 3 main steps:

1. nonlinear finite element analysis of the full structure,
2. selection of critical domains for post-processing and displacement field extraction on the boundaries,
3. discrete element analysis of the critical domains using the previous displacements field history.

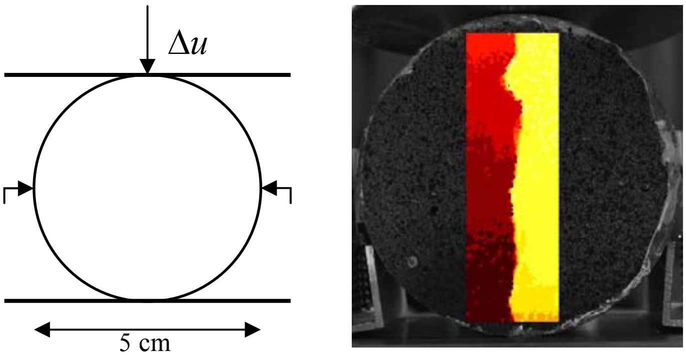

Figure 4. Experimental sketch (left) for the brazilian induced tension tests. Experimental displacement field by image processing (right).

4.2 *Concrete specimen case study*

To emphasize the ability of such a procedure for describing cracks' openings, a simple case study, widely described in the literature, has been selected. An induced tension test (Brazilian test) is treated accordingly to the three steps procedure. A sketch of the experimental set-up is presented in figure 4 as well as the strain field measured obtained by digital images correlation. The displacement discontinuity along the crack can be directly observed. The experiment is displacement-controlled. Two LVDT transducers measure the horizontal displacement. The crack opening in the center is observed through image processing.

4.3 *Finite element analysis*

The Brazilian test has been simulated using a coarse mesh (Fig. 5) and the scalar damage model described in the first section. The discretization uses 8 nodes cubic elements. Comparisons with the experimental responses are given in Figure 6. The computations have been performed under lateral displacement control. Nonlocal integral procedure has been used with an internal length of 1 cm.

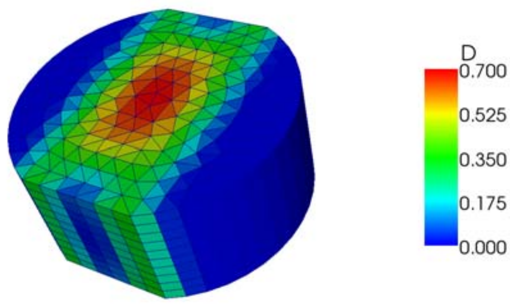

Figure 5. Damage field using a finite element coarse mesh and a continuum damage mechanics model.

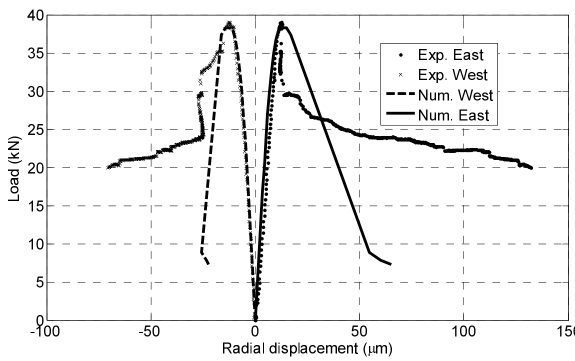

Figure 6. Comparison between experimental and numerical results (finite element model).

The critical zones clearly appear in the center of the specimen. If continuum damage mechanics models are able to globally recover the structural response of the specimen (load displacement curve, damage pattern), the link with the refined crack description is quite difficult to assess, depending on the internal length chosen for the analysis.

4.4 *Discrete element post processing*

From the finite element results, the central area can be selected for the discrete element post processing. The 3D displacement field obtained from the nonlinear finite element analysis at the peak load is therefore used as boundary conditions for the discrete element computation. Due to the difference in meshes density, linear interpolation is used to obtain the displacement field at each node of the refined discrete mesh. The 2D and 3D discrete element meshes are presented in the Figure 7. The rectangular central area can be observed as well as the mesh refinement due to Voronoi cell meshing.

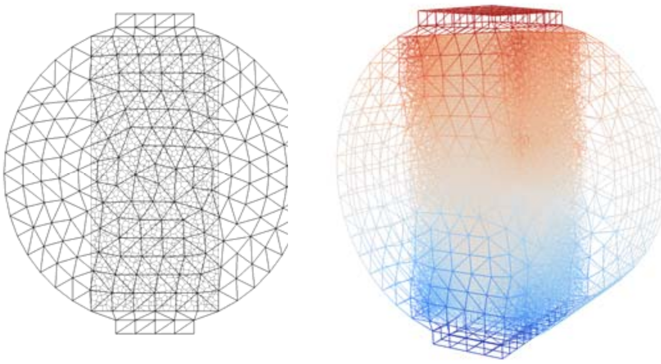

Figure 7. Discrete elements mesh in the central area.

Figure 8 plots the crack opening in the concrete core obtained from the discrete element method. At the peak load, corresponding to a maximum value for the damage variable equal to 0.7, a maximum crack opening of 3.3μm is calculated. For comparison, the experimental average crack opening is obtained by subtracting the elastic part of the behaviour (Boulay *et al.* 2009). At the peak load, a crack opening equal to 3.6μm has been measured, in full agreement with the numerical results.

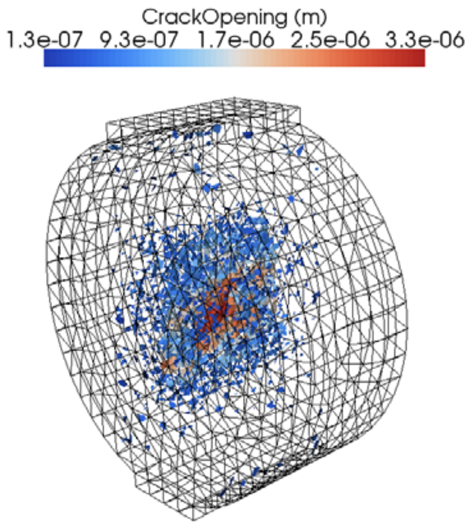

Figure 8. Crack opening distribution in the central part of the concrete specimen (peak load).

5 CONCLUSIONS AND OUTLOOK

Quantifying cracking in reinforced concrete structure still remains an important and difficult task. Among all the different existing approaches (discrete, continuous, X-FEM), the present paper proposes a coupled finite/discrete element approach. Its principle lies in two distinct steps. First, a coarse finite element analysis is performed in order to locate areas where crack propagation is intensive. Second, based on the knowledge of the displacement field computed at the areas boundaries, a discrete element analysis is performed. Local information regarding cracks' pattern can be obtained at a lower computational cost. A continuum mechanics damage-based model is first presented. Such a model is successful in describing the global structural behavior of cracked reinforced concrete elements. The discrete element post-processor is then focused on critical zones from the previous analysis. A Brazilian test is considered as a structural case study. Quantitative results, expressed in terms of load/displacement, match satisfyingly the experimental measurements. Discrete analysis leads to very accurate numerical results in terms of mean crack opening. These first results demonstrate that coupled finite/discrete element approach can be tuned as a powerful tool for crack propagation problems. They are very promising for further studies.

REFERENCES

Bazant Z.P., Tabbara M.R., Kazemi M.T. & Pijaudier-Cabot G. 1990. Random particle model for fracture of aggregate and fibre composites, *Journal of Engineering Mechanics* ASCE 116(8): 1686-1705.

Belytschko T. & Black T. 1999. Elastic crack growth in finite elements with minimal remeshing, *International Journal of Numerical Methods in Engineering* 45(5): 601-620.

Belytschko T., Fish J. & Engelman B.E. 1988. A finite element with embedded localisation zones, *Computer Methods in applied Mechanics and Engineering* 70: 59-89.

Bolander J.E. & Saito S. 1998. Fracture analysis using spring networks with random geometry, *Engineering Fracture Mechanics* 61: 773-780.

Boulay C., Dal Pont S., Delaplace A., Delahousse H. & Tailhan J.L. 2009. An experimental test for cracking concrete under controlled conditions. *ICF 12 - 12th International Conference on Fracture.*

D'Addetta G.A., Kun F. & Ramm E. 2002. On the application of a discrete model to the fracture process of cohesive granular materials, *Granular Matter* 4: 77-90.

Delaplace A. & Ibrahimbegovic A. 2006. Performance of time-stepping schemes for discrete models in fracture dynamic analysis, *International Journal for Numerical Methods in Engineering* 65(9): 1527-1544.

Delaplace A. & Desmorat R. 2007. Discrete 3d model as complimentary numerical testing for anisotropic damage, *International Journal of Fracture* 148: 115-128

Delaplace A. 2009.Tensile damage response from discrete element virtual testing, *Geomechanics and Geoengineering* 4:79-89

Dragon A. & Mroz Z. 1979. A continuum model for plastic-brittle behaviour of rock and concrete, *International Journal of Engineering of Science* 17: 121-137.

Gabet T., Malécot Y. & Daudeville L. 2008. Triaxial behaviour of concrete under high stresses: Influence of the loading path on compaction limit states, *Cement and Concrete Research* 38:403-412.

Larsson R. & Runesson K. 1996. Element embedded localisation band based in regularised displacement discontinuity, *Journal of Engineering Mechanics* ASCE 122: 402-411.

Mazars J. 1984. Application of damage mechanics to concrete structures non linear modeling (in French), Thèse d'Etat Université Paris 6.

Moes N., Dolbow J. & Belytschko T. 1999. A finite element method for crack growth without remeshing, *International Journal of Numerical Methods in Engineering* 46: 131-150.

Moukarzel C. & Herrmann H. 1992. A vectorizable random lattice, *J. Stat. Phys*. 68:911-923

Oliver J. 1996. Modelling strong discontinuities in solid mechanics via strain softening constitutive Equations. Part I: Fundamentals, *International Journal of Numerical Methods in Engineering* 39: 3575-3600.

Pensée V., Kondo D. & Dormieux L. 2002. Micromechanical analysis of anisotropic damage in brittle materials, *J. Eng. Mech*. ASCE 128(8): 889-897.

Pijaudier-Cabot G. & Bazant Z.P. 1987. Nonlocal damage theory, *J. Eng. Mech.* ASCE 113: 1512-1533.

Ragueneau F., La Borderie Ch. & Mazars J. 2000. Damage Model for Concrete Like Materials Coupling Cracking and Friction, Contribution towards Structural Damping: First Uniaxial Application. *Mechanics Cohesive Frictional Materials* 5: 607-625.

Schlangen E. & Garboczi E.J. 1997. Fracture simulations of concrete using lattice models: Computational aspects. *Eng. Fracture Mechanics* 57(2/3): 319-332

Simo J.C. & Ju J.W. 1987. Strain and stress based continuum damage models—I formulation. *Int J Solids Struct.* 23: 821-40.

Van Mier J.G.M., Van Vliet, M.R.A. & Wang T.K. 2002. Fracture mechanisms in particle composites: statistical aspects in lattice type analysis. *Mech. Mater*. 34: 705-724

Willam K.J., Pramono E. & Sture S. 1987. Classification of smeared crack models based on material and structural properties, *Int. J. Solids Structures* 35(12): 1289-1308.

Xiao S. & Belytschko T. 2004. A bridging domain method for coupling continua with molecular dynamics. *Computer methods in applied mechanics and engineering* 193:1645-1669.